JOINT EUROPEAN TORUS JET

JET–P(87)12

B.J.D. Tubbing, N. Lopes Cardozo, M.J. van der Wiel
and the JET Team

Tokamak Heat Transport A Study of Heat Pulse Propagation in JET

Tokamak Heat Transport A Study of Heat Pulse Propagation in JET

B.J.D. Tubbing[1], N. Lopes Cardozo[1], M.J. van der Wiel[1]
and the JET Team

JET-EFDA, Culham Science Centre, OX14 3DB, Abingdon, UK

[1]FOM-Instituut voor Plasmafysica 'Ri jnhuizen', Nieuwegein, The Netherlans

Preprint of Paper to be submitted for publication in
Nuclear Fusion

Abstract

The propagation of heat pulses originating from sawtooth activity in JET has been investigated in a series of limiter discharges with the parameters $I_p \simeq 3MA$, $B_T \simeq 3T$, $\kappa = 1.45$. The auxiliary power was varied, so that the total power ranged from 2 to 13.5 MW.

Electron temperature perturbations in a 20 cm region around a minor radius $r = \frac{2}{3}a$. were recorded with high time resolution, using a 12 channel electron cyclotron emission (ECE) polychromator. From these measurements the electron heat diffusivity χ_e^{HP} was derived.

Over the the whole range of powers considered, χ_e^{HP} was found to be independent of power and to lie in the range 2.5 ± 0.5 m^2/s. We compare χ_e^{HP} to χ_e^{GLO} derived from global power balance analysis. For ohmic heating the latter is lower than χ_e^{HP} by a factor 2.5. For increasing auxiliary power, χ_e^{GLO} approaches χ_e^{HP}.

We present a model for the dependence of the local χ_e on the temperature gradient, which permits a unified description of the heat pulse behaviour, the deterioration of confinement and a certain degree of profile consistency. The model does not invoke non-local parameters like the total power input.

It is shown that the present heat pulse data contradicts τ_E-scaling laws of the typical form $\tau_E \div P^{-0.5}$.

Section 1 Introduction

Anomalous electron heat conduction is one of the main loss mechanisms in present day tokamaks. There are two classes of experimental methods to assess the electron heat diffusivity, χ_e. The first, the analysis of the steady state power balance is a static method. It usually suffers from a lack of knowledge of the amount of power transported via the ions and of the power deposition profiles. Still, with reasonable assumptions, a global estimate for χ_e can be obtained. The second class involves dynamic methods, ie. the analysis of the radial diffusion of a local perturbation of the electron temperature profile. This perturbation can be either actively imposed, or it can be due to a sawtooth collapse. In the latter case the process is usually referred to as heat pulse propagation [1,2]. We shall adopt this term, though it should be noted that the process is diffusive [2,3]. There is no energy carrying propagating heat pulse as there would be, were the transport wave-like or ballistic.

Generally the value for χ_e derived from heat pulse analysis, χ_e^{HP}, is found to exceed the value χ_e^{GLO} derived from a global power balance analysis. This discrepancy ranges from a factor 1-4.(T10,FT,ISX-B,JET, refs 3-7) to up to a factor 20 (TFTR, ref.8). In previous publications a satisfactory explanation for the discrepancy could not be given, except by invoking an inward heat flow by an unknown mechanism [8].

The present paper aims at obtaining an understanding of the discrepancies found between χ_e^{GLO} and χ_e^{HP}. We present new measurements of χ_e made at JET, derived from both power balance analysis and heat pulse studies. The main line of research was to investigate the behaviour of χ_e under conditions of strong additional heating. To that end discharges with total power input ranging from 2.1 to 13.5 MW have been studied. In the discharges with the highest level of additional power, the latter exceeds the ohmic dissipation by

a factor of six, and the confinement is degraded by a factor of three with respect to ohmic discharges. On the theoretical side, we re-examine in detail the relation between the static and dynamic estimates of χ_e.

We introduce the incremental heat diffusivity, χ_e^{inc}, and determine this quantity in three independent ways: from heat pulse propagation measurements, from a global power balance analysis, and from a local power balance analysis

This concept turns out to be fruitful in that it solves the discrepancies observed between χ_e^{GLO} and χ_e^{HP}, and it leads to a model for χ_e which is capable of describing the heat pulse measurements, confinement degradation and a certain amount of profile consistency.

Section 2 χ_e derived from power balance analysis

In a general form the heat flow per unit area, Q, can be written as a sum of conductive and convective parts:

$$Q = - \chi_e n_e \nabla_r T_e + \frac{5}{2} n_e T_e v_{conv}$$

Since there are no indications, either experimental or theoretical, that a convective flow plays a role of any importance in transport, we will neglect this term. Then χ_e is locally defined as:

$$\chi_e = - \frac{Q}{n_e \nabla_r T_e}$$

Note that within this definition χ_e can well be a function of local plasma parameters like n_e, T_e or $\nabla_r T_e$. An estimate for χ_e at $r = \frac{2}{3}a$ can be obtained from the global power balance, using

$$\chi_e^{GLO} = \frac{ab}{4\tau_E} \qquad (1)$$

where τ_E is the global energy confinement time, defined by $\tau_E \equiv W/P$; here W is the total kinetic energy content and P is the total input power. This expression is derived for parabolic profiles of T_e and n_e, and with the assumption that $P/W \approx P_e/W_e$, where P_e and W_e denote the power conducted by and the energy stored in the electrons. Deviations from these assumptions only slightly change the numerical factor ab/4.

In Fig. 1[a] W is plotted versus P, for a selection of limiter discharges with combined neutral injection and ICRH additional heating which

are not radiation dominated, with I_p=3 MA, B_T=3.4 T, n_e=(2-3)10^{19} m^{-3}. It appears that the data can be represented by an off-set linear scaling of W with P [9,10]:

$$W = W_o + \tau_E^{inc} P \tag{2}$$

The incremental energy confinement time $\tau_E^{inc} \equiv \frac{dW}{dP}$ is clearly different from the more familiar τ_E (see Fig 1^b).

In analogy to τ_E^{inc} we define the incremental heat diffusivity by

$$\chi_e^{inc} = \frac{1}{n_e} \frac{dQ}{d\nabla_r T_e}\Big|_{n_e = \text{constant}} \tag{3}$$

Note that the derivative is taken while keeping n_e constant. With this definition it is possible to derive the analog of Eq.(1):

$$\chi_e^{inc} = \frac{ab}{4\tau_E^{inc}} \tag{4}$$

which again holds around r = $\frac{2}{3}$a. The experimental data shown in Fig 1^a yield τ_E^{inc} = 210 ms, from which we derive

$$\chi_e^{inc} = 2.6 \pm 0.5 \ m^2/s$$

The error quoted reflects the uncertainty in the estimate of the electron fractions of W and P.

In an alternative approach we can obtain a local value for χ_e^{inc}. By plotting directly the local heat flow Q versus the local T_e-gradient, we can determine χ_e^{inc} as the slope $\frac{1}{n_e} \frac{dQ}{d\nabla_r T_e}$. We perform this analysis again at minor radius

$r = \frac{2}{3}a$, for the following reasons:

- In the region $r < \frac{2}{3}a$ radiative losses are negligible, while $\gtrsim 75$ % of the input power is deposited in this region. Therefore an estimate of the conducted power can be quite accurate.
- $r = \frac{2}{3}a$ is in the confinement region, where heat transport may be supposed to be diffusive.
- the heat pulse measurements are performed around $r = \frac{2}{3}a$.

In Fig.2[a] $\nabla_r T_e$ is plotted versus P/n_e, for constant n_e. Q is proportional to P, according to

$$Q.S = P_e(r < \tfrac{2}{3}a) \approx 0.5\ P$$

where S denotes the area of the flux surface at $r = \frac{2}{3}a$. The values for $\nabla_r T_e$ are averaged over the flux surface.

Again the data set can be represented by an off-set linear scaling. We find a second determination of χ_e^{inc}:

$$\chi_e^{inc} = 2.5 \pm 0.7\ m^2/s$$

The error now also contains uncertainties in the determination of the local temperature gradient and the local density.

We have thus found two consistent estimates for χ_e^{inc} from power balance analysis. It appears that χ_e^{inc} is a useful concept, since it represents the heat conduction properties of the electrons over a wide range of input power.

The observation that Q as a function of $\nabla_r T_e$ is not a straight line through the origin implies that χ_e is a function of $\nabla_r T_e$ as is shown in Fig. 2[b]. This dependence of χ_e on $\nabla_r T_e$ may be implicit (eg. a parametrical dependence on the current density profile) or explicit (eg. micro turbulence being driven directly by $\nabla_r T_e$). The crucial difference between an implicit and an explicit

dependence is the time scale involved. Since power balance analysis is performed only in steady states, from this type of analysis we can get no knowledge about the nature of the dependence. However, a study of the dynamic behaviour of Q as a function of $v_r T_e$ will bring out the difference. Heat pulse propagation analysis is an appropriate method here, since in it only the T_e-profile is perturbed, leaving all other plasma parameters fixed, and the time scale of the process is typically 10 ms, compared to $\tau_E \approx 500$ ms and the resistive skin time $\tau_R \approx 10$ s.

It should be noted, finally, that an alternative interpretation of the dependence shown in Fig 1[a] is possible. We can rewrite Eq.(2) in the form:

$$W = \tau_E^{inc} (P + P_o) \qquad (5)$$

where P_o $(= W_o/\tau_E^{inc})$ should then be taken to represent a constant 'heat pinch' term [8]. Its value is 5 MW. In this interpretation the net heat transport is the result of an outward diffusive flow, with $\chi_e = \chi_e^{inc}$, counteracted by an inward flow which is independent of parameters like n_e , T_e or P. No theory exists at the present time which claims to describe a mechanism for such a heat pinch.

Section 3 Heat pulse propagation analysis

3.1 Theory

Heat pulse propagation is the process in which an initially localised temperature perturbation gives rise to a delayed temperature excursion elsewhere in the plasma. In our case the initial T_e-perturbation is due to a sawtooth collapse. Fig.3 presents in schematic form the evolution of the T_e-profile during sawtoothing, and defines the heat pulse delay time $t_p(r)$ and the amplitude A(r). As we have published elsewhere [11], for a cylindrical plasma the relation between χ_e^{HP} and the measured quantities t_p and A is given by

$$\chi_e^{HP} = 4.2 \frac{a v_{HP}}{\alpha} \qquad (6)$$

where a denotes the minor radius (of the circular plasma), the heat pulse velocity is defined by $v_{HP} \equiv (\frac{d}{dr} t_p)^{-1}$ and the radial damping rate is defined by $\alpha \equiv 10a \frac{d}{dr} \log A$, and is expressed in dB.

As we show in the Appendices, allowing χ_e to be a function of $\nabla_r T_e$ implies that theoretically χ_e^{HP} is defined by:

$$\chi_e^{HP} \equiv \frac{1}{n_e} \frac{\partial Q}{\partial \nabla_r T_e}$$

This is an important improvement on the standard treatment, which assumes that $\chi_e^{HP} = Q/n_e \nabla_r T_e$. We also show that a T_e-dependence in χ_e does not have a significant effect on the determination of χ_e^{HP}. Hence , if χ_e is not an explicit function of T_e, χ_e^{HP} and χ_e^{inc} are identical by definition. Consequently χ_e^{HP} should not be compared to χ_e^{GLO} as has been the common practice up to now, but to χ_e^{inc} instead. It should be remarked, again, that a $\nabla_r T_e$ dependence in χ_e only affects the heat pulse process if it acts on a millisecond time scale.

3.2 Diagnostic and data processing

The JET far infrared grating polychromator [5,12] measures the electron cyclotron emission in the second harmonic extraordinary mode, at twelve radial positions along a line of sight in the median plane of the plasma simultaneously. For the type of discharges discussed here, thermal equilibrium has been well established, so that the emission can be taken to be linearly proportional to the electron temperature.

The 12 channels cover a radial region of roughly 60 cm; the spatial resolution is about 5 cm along the line of sight and 15 cm FWHM in the perpendicular direction. The noise level depends on the toroidal field, the electron cyclotron emission intensity being proportional to the square of the frequency. At B_T = 3T, f = 168 GHz, the typical noise equivalent temperature is 30 eV, at an electrical bandwidth of 10 kHz.

The instrument is calibrated against a Michelson interferometer[13,14], which in turn has been absolutely calibrated using a large area black body [15]. The temperatures thus obtained agree with those from Thomson scattering normally to within 10 % [15]. Fig. 4 shows an example of the raw data for radial positions in the confinement region. The noise is pure detector noise, plasma noise is not observed.

To improve the S/N ratio of the signals, we apply a coherent addition procedure to a series of sawteeth within one discharge. The procedure is as follows: we select a time window of typically 2 seconds during the flat top and during a period of constant auxiliary heating power. The precise times of the sawtooth collapses in the selected time window are determined from one of the signals originating from inside the mixing radius. Intervals of the order of 100 ms are set around each sawtooth collapse, and the signals are added coherently, ie. using the collapse as the time trigger. The gain in S/N achieved is equal to the square root of the number of sawteeth added.

Figure 5 shows the result of the procedure applied to 22 sawteeth in a 2.5 s time window for the discharge shown in Fig 4. The procedure is justified under

the assumption that the process of heat pulse propagation is independent of sawtooth amplitude and duration. These assumptions have been validated by confirming the agreement between heat pulse parameters for individual, high S/N ratio, sawteeth and those averaged over a series of sawteeth.

From signals as shown in Fig. 5 we determine values of the delay time $t_p(r)$ and for the amplitude A(r) (see Fig.3). The t_p and A values corresponding to the signals of Fig. 5 are shown in Fig. 6. The t_p data points have error bars of typically $\leq$ 20%. This precludes an accurate determination of the radial behaviour of t_p. From Fig.6 we can readily determine the heat pulse velocity $v_{HP}^{\dagger}$ and the radial damping rate $\alpha^{\dagger}$ as measured along the chord in the horizontal midplane on the outside of the plasma.

In order to permit application of Eq.(6), which is derived for a cylindrical plasma, $v_{HP}^{\dagger}$ and $\alpha^{\dagger}$ need to be converted to flux surface averaged values, ie. we must correct for the Shafranov shift (s) and the elongation (κ) of the plasma. The corrected values are given by:

$$v_{HP} = \sqrt{\kappa}\,\frac{a}{a-s}\,v_{HP}^{\dagger} = \sqrt{\kappa}\,\frac{a}{a-s}\,\left(\frac{d}{dr}t_p\right)^{-1}$$

$$\alpha \;=\; \frac{a-s}{a}\,\alpha^{\dagger} \;=\; 10(a-s)\frac{d}{dr}\log(A)$$

3.3 Results

The data set of the power scan comprises a total of 25 observations, with total power input up to a level of 13.5 MW. Some pulses were analysed before, during and/or after the time window of auxiliary heating.

An important constraint on the data is that the density and input power are correlated as shown in Fig 7: upon raising the input power by a factor of 6, the density increases by a factor of 2.5. The basic plasma parameters for the discharges analysed in this paper are given in Table 1.

TABLE 1

Parameter Range of Analysed Discharges

Toroidal field	(T)	2.9 - 3.5
Plasma current	(MA)	2.7 - 3.0
Elongation		1.4 - 1.5
Safety factor q_Ψ		4.8 - 6.3
Input power	(MW)	2.1 -13.5
Density	($10^{19} m^{-3}$)	2.1 - 4.7

The values for χ_e^{HP} obtained for these discharges are plotted in Fig. 8 as a function of total input power. For comparison also the trend of χ_e^{GLO}, corresponding to the fit to the data in Fig.1[a], is plotted. The dashed lines depict a τ_E-scaling, which is discussed in Sec. 4.3

We observe that the experimental χ_e^{HP} does not depend measurably on input power, but has a rather constant value of 2.4 ± 0.5 m^2/s. The error quoted reflects the experimental uncertainties in v_{HP} and α.

To illustrate that the level of input power does not affect the heat pulse, Fig. 9 compares the heat pulses at six radial positions, for two discharges, with 2.7 and 10.4 MW total input power respectively. While the input power is quadribled, the heat pulses have not changed.

Section 4 Interpretation and discussion.

4.1 Introduction

As the main points of the previous sections, we have found that:

a) Analysis of the power balance yields $\chi_e^{inc} = 2.5 \pm 0.5$ m^2/s, and shows that χ_e is a function of $\nabla_r T_e$, either implicitly or explicitly. For the same series of discharges χ_e^{GLO} varies from 0.7 to 2 m^2/s

b) analysis of heat pulse measurements yields $\chi_e^{HP} = 2.5 \pm 0.5$ m^2/s, independent of input power.

c) inspection of the mathematics of the diffusion process shows that if the dependence of χ_e on $\nabla_r T_e$ is explicit, ie. acting on a ms time scale, and χ_e does not depend explicitly on T_e, then $\chi_e^{HP} \equiv \chi_e^{inc}$ by definition.

We interpret the observed agreement between χ_e^{inc} and χ_e^{HP} as confirming that the two quantities are identical. This observation has several consequences. Firstly it implies a specific relation between χ_e and $\nabla_r T_e$, which may be linked to anomalous transport theory. This is discussed in Sec. 4.2. Secondly, it implies that measuring χ_e^{HP} is a direct way to assess τ_E^{inc}, and as such is a critical test of scaling laws for τ_E. Thirdly, the proposed model for χ_e may provide an explanation for discrepancies between χ_e^{GLO} and χ_e^{HP} observed in other experiments. Some instances are discussed in Section 4.4. Section 4.5 deals with the properties of the model in the view of the concept of profile consistency.

4.2 A model for χ_e

The present data set for χ_e from power balance analysis spans only a limited range of temperature gradients (see Fig. 2). Due to the high ohmic heating powers in JET, there are no data points below 3 keV/m. For the range of $\nabla_r T_e$ where we do have data, the off-set linear fit shown in Fig. 2 implies that χ_e is a function of $\nabla_r T_e$ of the form:

$$\chi_e = \chi_{e,low} + (\chi_e^{inc} - \chi_{e,low})\left(1 - \frac{\nabla_r T_{e,crit}}{\nabla_r T_e}\right) H(\nabla_r T_{e,crit} - \nabla_r T_e)$$

This 'critical gradient' model is sketched in Fig 10. At high gradients χ_e approaches a saturation value which is equal to χ_e^{inc}. We speculate that below a certain critical temperature gradient, $\nabla_r T_{e,crit}$, χ_e approaches a low, eg. neo-Alcator value, $\chi_{e,low}$. This regime may well be outside the normal operational parameter space of JET or most tokamaks.

It should be noted that other dependences of χ_e on $\nabla_r T_e$, like $\chi_e \div \nabla_r T_e$ are not compatible with the heat pulse data and the off-set linear fit of Q/n_e vs $\nabla_r T_e$, or W vs. P (see also Sec. 4.3 and 4.4).

The sketched behaviour could be interpreted to indicate that above the critical $\nabla_r T_e$ a micro-instability sets in, which saturates at higher values of $\nabla_r T_e$. χ_e^{inc} accordingly makes a more or less discontinuous transition from a low neo-Alcator value to a value of 2.5 m^2/s for the present conditions. Further study is required to establish whether one of the various instabilities proposed theoretically has these characteristics.

Two remarks should be made. First it may well be that the pressure gradient is the critical parameter rather than the temperature gradient. Since in heat pulse measurements n_e is fixed, this does not show up in the analysis. Second, it seems reasonable that the gradients involved should be taken with respect to Ψ rather than radius. In fact this has been tacitly assumed when we transformed our data from the D-shaped, Shafranov shifted geometry to the circular, concentrical geometry to allow comparison with the cylindrical diffusion model. For the present data set this has no further implications, since the plasma cross-section was not varied significantly

The proposed model for χ_e consistently accounts for the heat pulse results and for the behaviour of W as a function of P. It should be noted that it uses

local parameters only, no non-local parameter like total input power occurs in the expression for χ_e. In steady state, local and non-local parameters are strictly coupled, and a study of different plasma equilibrium states cannot reveal wether heat transport is governed by local processes or not. The study of the transient process of heat pulse propagation , however, indicates that indeed heat transport in JET can be described as a purely local phenomenon. Numerical simulation studies will be undertaken to investigate whether the above χ_e model is also capable of describing other transients such as the switch-on of ICRH power or the injection of a pellet.

4.3 Implications for τ_E-Scalings

The ability of heat pulse analysis to derive values of χ_e^{inc}, and hence τ_E^{inc}, allows us to examine various τ_E-scaling laws more critically than is possible on the basis of power balance analysis. We consider the family of scaling laws of the form:

$$\tau_E = \text{constant } P^{-\gamma}$$

where the constant may contain global plasma parameters. The value of γ is usually around $\gamma = 0.5$ (eg.the Goldston L-mode scaling [16]). τ_E^{inc} follows from

$$\tau_E^{inc} = \frac{\partial W}{\partial P} = \frac{\partial}{\partial P}(\tau_E P) = (1 - \gamma)\tau_E$$

and hence

$$\chi_e^{inc} = \frac{1}{1-\gamma}\chi_e$$

Clearly with this type of scaling law χ_e^{inc} would have the same dependence on P as χ_e as shown in Fig.8 for γ=0.5. Clearly a constant value of χ_e^{inc}, independent of power, is a better fit to the χ_e^{HP} measurements, even allowing for the relatively large error bars on the data points.

4.4 The Discrepancy between χ_e^{GLO} and χ_e^{HP}

The χ_e model presented above can generally account for the discrepancies between χ_e^{GLO} and χ_e^{HP} found on other tokamaks. The TFTR data follow the same general trend that the discrepancy is smallest for large χ_e^{GLO}, but ref [8] does not give enough details of the discharge conditions to investigate this closer. It may be noticed that, in the χ_e-model, the steeper the rise of χ_e as a function of $\nabla_r T_e$, the larger is the difference between χ_e^{inc} and χ_e^{GLO}. Moreover, in that case χ_e^{inc} decreases for increasing χ_e^{GLO}, which indeed appears to be the trend in the TFTR data. Still, the factor of 20 difference found on TFTR is hard to explain purely in terms of the model. The factor 1 to 4 found in most experiments is perfectly plausible, though.

Heating studies in ISX-B [3] showed a considerable increase of χ_e^{HP} when going from ohmic to auxiliary heated conditions. This might be understood as ohmic heating only produced gradients below critical, whereas the auxiliary heating drove $\nabla_r T_e$ beyond the critical value.

Furthermore, it was found in ECRH experiments on TFR [17], that the additional power could raise $\nabla_r T_e$ in the central region by very large factors, whereas χ_e appeared to increase by a modest amount only. We interpret this in terms of the relatively small difference between χ_e below the critical $\nabla_r T_e$ and its saturation value.

Finally, we note that although the above conclusions lead to a consistent picture of a variety of observations, the experiment does not provide a basis on which to distinguish between a $\nabla_r T_e$ dependence of χ_e and the case of a constant χ_e plus a constant power pinch (see Sec.2). Only measurements at sub-critical values of $\nabla_r T_e$ could bring out the difference between the two models. In this light the following observation is of interest.

First results from pellet fuelled JET discharges [23] show a marked drop of χ_e^{HP} during a period of $\approx$0.5 second immediately following the pellet injection. The interpretation is difficult since many effects may play a role, but we note

that during this period the T_e-gradient in the confinement region is strongly reduced due to the cooling brought about by the pellet: $\nabla_r T_e$ falls from 4 to 2.5 keV/m. We may tentatively say that this observation is thus in agreement with the above χ_e model rather than the constant power pinch model.

4.5 Profile Consistency

Finally, we consider the consequences of our χ_e-model for the issue of profile consistency. The concept is based on observations made on many machines that the temperature profile does not seem to depend strongly on the level of input power. This has been interpreted in terms of a dependence of χ_e on non-local variables like eg. the total power input [18,19]. However, it can be shown that the purely local χ_e-model proposed here also leads to some degree of profile consistency: if the local heat diffusivity increases with increasing temperature gradient, this results in an apparent insensitivity of the electron temperature profile to additional localized power input. Thus, it seems unnecessary to complicate the understanding of χ_e by invoking a dependence on non-local parameters.

Section 5 Conclusions

In conclusion we have found that, for the data set considered, χ_e^{HP} is constant within the measuring accuracy of 20%. In particular no dependence on input power is found. A 'critical gradient' model for χ_e is presented which provides a unified description of the dynamic heat pulse measurements and the results from static power balance analysis. In this model the heat flow is purely locally determined, by a heat diffusivity which itself is a function of the temperature gradient. This can be interpreted to indicate that some anomalous transport mechanism sets in when the temperature gradient exceeds a critical value, and gradually saturates at higher T_e-gradients. A necessary condition is that this mechanism can react to changes of the T_e-profile within a few milliseconds.

Furthermore we have shown that an off-set linear dependence of the kinetic energy content on the total input power agrees well with the heat pulse data, while the latter is at variance with scaling laws of the form $\tau_E \div P^{-\gamma}$.

ACKNOWLEDGEMENTS

The authors are indebted to Dr H Piekaar, who initiated the heat pulse work at JET, and to Ing T Oyevaar for keeping the polychromator in perfect working condition. It is a pleasure to acknowledge the many lively and stimulating discussions we had with Drs J Callen, J Cordey, J Christiansen and P Thomas. We thank Drs A Taroni and F Tibone for making results from the full transport simulation code JETTO available to us in a suitable form, and for the enlightening discussions on the subject of heat transport. We thank Dr W Goedheer from the FOM-Institute 'Rijnhuizen' for his help with the cylindrical diffusion code. We also want to express our gratitude to the Electron Temperature Group at JET, in particular to Drs A Costley, D Campbell, D Bartlett and to H Bindslev, and to Dr P Stott for his comments on the manuscript.

The authors are attached JET-staff, under a task agreement between FOM and JET. This work was performed as part of the research programme of the association agreement of Euratom and the 'Stichting voor Fundamenteel Onderzoek der Materie' (FOM) with financial support from the 'Nederlandse Organisatie voor Zuiver-Wetenschappelijk Onderzoek' (ZWO) and Euratom.

Appendix A

In this appendix we investigate the mathematics of the heat pulse. The approach is along lines set out by Callen and Jahns [1], but differs in that we take into account

- T_e and $\nabla_r T_e$ dependences in χ_e
- perturbed source and sink terms

By subtracting the steady state transport equation from the perturbed equation, we arrive at the basic equation governing the diffusion of the T_e-perturbation:

$$\frac{3}{2}\frac{d}{dt}(n_e\tilde{T}_e) = -\nabla.\tilde{\mathbf{Q}} + \tilde{P} \qquad (A1)$$

where Q is the heat flow per unit area and P is the source power density, ie. ohmic dissipation plus ion-electron energy exchange less any radiative losses. Quantities with a tilde are perturbations with respect to the equilibrium value, eg. $\tilde{Q} = Q - Q_{eq}$. Q is related to $\nabla_r T_e$ via:

$$Q = -n_e\chi_e\nabla_r T_e$$

Allowing χ_e to be a function of T_e and $\nabla_r T_e$ yields, to first order of perturbed quantities:

$$-Q = n_e\tilde{\chi}_e\nabla_r T_e + n_e\chi_{e,eq}\nabla_r\tilde{T}_e$$

$$= n_e\chi_e^{HP}\nabla_r\tilde{T}_e + n_e\left(\frac{\partial\chi_e}{\partial T_e}\right)(\nabla_r T_e)\tilde{T}_e \qquad (A2)$$

with

$$\chi_e^{HP} = \chi_{e,eq} + \left(\frac{\partial\chi_e}{\partial\nabla_r T_e}\right)\nabla_r T_e \qquad (A3)$$

The thus defined χ_e^{HP} is the quantity that eventually is derived from heat pulse analysis. We see that:

- A $\nabla_r T_e$-dependence in χ_e replaces $\chi_{e,eq}$ by χ_e^{HP}, but retains the diffusive nature of the heat pulse;
- A T_e-dependence in χ_e adds a term to $\tilde{Q}$ which has the form of a convective heat flow. This term mainly affects the radial behaviour of the amplitude of the heat pulse. As is shown in Appendix B, the effect on the determination of χ_e^{HP} is small, except for very strong T_e-dependences. For ohmic JET discharges, $\chi_e \div T_e$ would give rise to a 15% overestimate of χ_e^{HP}. Stronger dependences are incompatible with the results of power balance analysis.

Taking then that χ_e has no explicit T_e-dependence, substitution of Eq.(A2) in (A1) yield a damped diffusion equation:

$$\frac{3}{2} n_e \dot{\tilde{T}}_e = \nabla.(n_e \chi_e^{HP} \nabla_r \tilde{T}_e) - \frac{n_e}{\tau_d} \tilde{T}_e \qquad (A4)$$

Here $\tilde{P}$ has been linearized in $\tilde{T}_e$, by defining the characteristic damping time constant $\tau_d \equiv n_e (\frac{\partial}{\partial T_e} P)^{-1}$

To model the heat pulse propagation process Eq.(A4) is solved numerically in cylindrical geometry. In previous work on heat pulse propagation τ_d is always implicitly taken equal to infinity, ie. much longer than the duration of the relaxation process. As was shown by Goedheer [21], this condition is not always satisfied. At JET, where τ_d is typically of the same order as a sawtooth period, the assumption would demonstrably lead to incorrect results. However, we haven shown recently [11] that this problem can be solved by using experimental information from both the delay time $t_p(r)$ and the amplitude $A(r)$,

rather than only $t_p(r)$. Ref [11] demonstrates that, when defining a heat pulse velocity $v_{HP} \equiv (\frac{d}{dt} t_p)^{-1}$ and a radial damping rate $\alpha \equiv 10a\frac{d}{dr}\log(A)$, χ_e^{HP} can be expressed as

$$\chi_e^{HP} = 4.2 \frac{a v_{HP}}{\alpha} \qquad (A5)$$

where a denotes the minor radius. This relation holds around $r = r_{mix} + 0.15a$ and the value of χ_e^{HP} thus derived is an average over the range $r_{mix} + 0.1a < r < r_{mix} + 0.2a$. The relation has been checked against full transport calculations and was found accurate. For the limiting case $\tau_d \rightarrow \infty$ expression (A5) coincides with the familiar result of Callen and Jahns [1], $\chi_e = (r^2 - r_{mix}^2)/8t_p(r)$. In JET conditions the latter expression is incorrect by about a factor 1.7. Using Eq.(A5) χ_e^{HP} can readily be deduced from the measured quantities v_{HP} and α.

Appendix B

In Appendix A we assumed $\frac{\partial\chi}{\partial T} = 0$ and found that our analysis then yields an experimental determination of χ^{HP} (in this appendix we drop the subscript 'e' for density of notation). In this appendix we address the question how big a systematic error could occur in this evaluation of χ^{HP} if $\frac{\partial\chi}{\partial T} \neq 0$.

Working out in cylindrical geometry the diffusion equation (A1) for the perturbed heat flow as given in Eq.(A2), we find:

$$\frac{3}{2}\dot{\tilde{T}} = \chi^{HP}\frac{\partial^2}{\partial r^2}\tilde{T} + \left[\frac{1}{n}\frac{\partial}{\partial r}(n\chi^{HP}) + \frac{1}{r}\chi^{HP} + (\frac{\partial\chi}{\partial T})(\frac{\partial T}{\partial r})\right]\frac{\partial\tilde{T}}{\partial r}$$

$$+ \left[\frac{1}{n}\frac{\partial}{\partial r}\{n(\frac{\partial\chi}{\partial T})(\frac{\partial T}{\partial r})\} + \frac{1}{r}(\frac{\partial\chi}{\partial T})(\frac{\partial T}{\partial r}) - \frac{1}{\tau_d}\right]\tilde{T} \quad (B1)$$

We write the extra terms due to $\frac{\partial\chi}{\partial T} \neq 0$ as

$$A = (\frac{\partial\chi}{\partial T})(\frac{\partial T}{\partial r})$$

$$B = \frac{1}{n}\frac{\partial}{\partial r}\{n(\frac{\partial\chi}{\partial T})(\frac{\partial T}{\partial r})\} + \frac{1}{r}(\frac{\partial\chi}{\partial T})(\frac{\partial T}{\partial r}) \quad (B2)$$

As we shall see, the effect of A is, for A>0, to anhance the radial damping rate α, without speeding up the heat pulse (the damping in this case is a function of radius rather than time, as opposed to the dissipative damping represented by τ_d). Since in determining χ^{HP} we use both v_{HP} and α, this may introduce a systematic error.

The extra term B, on the other hand, affects both v_{HP} and α analogously to the damping represented by τ_d. This type of damping is taken into account by the extended diffusive model, Eq. (A5). Hence the occurrence of B does not influence the evaluation of χ^{HP}.

We first concentrate on the effects of A. Clearly, the introduction of a spurious contribution to α, $\delta\alpha$, leads to a systematic error in the evaluation of χ^{HP}:

$$\chi^{HP}(\text{exp}) = \chi^{HP} \frac{\alpha(\text{exp}) - \delta\alpha}{\alpha(\text{exp})} \tag{B3}$$

where $\chi^{HP}(\text{exp})$ is the value of χ^{HP} derived from the measured quantities v_{HP} and $\alpha(\text{exp})$ using formula (6).

The effect of A on the damping rate was analysed by numerically solving Eq.(B1) for constant A. We found:

$$\delta\alpha \approx 4aA/\chi^{HP} \tag{B4}$$

($\delta\alpha$ in dB, a in m, A in m/s, χ in m^2/s). If we then take χ of the form $\chi \div T^{\gamma}$, (B2) and (B3) yield:

$$A = \gamma\chi\left(\frac{1}{T}\frac{\partial T}{\partial r}\right) \tag{B5}$$

and

$$\delta\alpha = 4\gamma\frac{\chi}{\chi^{HP}}\, a\left(\frac{1}{T}\frac{\partial T}{\partial r}\right) \tag{B6}$$

A typical average value of $a\left(\frac{1}{T}\frac{\partial T}{\partial r}\right)$ in the confinement region is, in JET (see ref [20]):

$$\left\langle a\left(\frac{1}{T}\frac{\partial T}{\partial r}\right)\right\rangle \approx -5$$

These estimates have been checked with the full simulation code JETTO [22]. A typical ohmic discharge was simulated twice, once with $\chi \div n^{-1}$ (Alcator-Intor scaling) and once with $\chi \div n^{-0.8} T^{-1}$ (Coppi-Mazzucato-Gruber scaling). The global value of χ was the same in both cases, and since no explicit $v_r T_e$-dependence is present, $\chi^{HP} \equiv \chi$ in these simulations. The result was $\delta\alpha$ = 20 dB, in good agreement with Eq.(B6). We therefore have some confidence that (B6) indeed is a useful estimate of $\delta\alpha$. v_{HP} was hardly different in the two cases.

To make the connection with the experiment we express the relative error made in the evaluation of χ^{HP} in terms of measured quantities, by combining (B3) and (B6):

$$\frac{\chi^{HP} - \chi^{HP}(exp)}{\chi^{HP}} = \frac{\delta\alpha}{\alpha(exp)} = \frac{\alpha^{\oplus}}{\alpha(exp) + \alpha^{\oplus}} \qquad (B7)$$

with

$$\alpha^{\oplus} = 4\gamma \frac{\chi}{\chi^{HP}(exp)} a\left(\frac{1}{T}\frac{\partial T}{\partial r}\right)$$

We shall now estimate i) the γ required to resolve a discrepancy $\chi/\chi^{HP}(exp) \approx 0.4$ as is observed in ohmic discharges, and ii) what the systematic error in χ^{HP} would be for a modest T-dependence.

In ohmic discharges we have typically $\chi/\chi^{HP}(exp) \approx 0.4$ and $\alpha(exp) \approx 45$ dB. To achieve $\chi^{HP} = \chi = 0.4\chi^{HP}(exp)$ we need, according to (B3):

$$\delta\alpha = -1.5\ \alpha(exp) \approx -70 \text{ dB}$$

and hence, using (B6)

$$\gamma = 9$$

Such a strong T-dependence is totally incompatible with observed T-profiles and power balance analysis, because it would imply an extremely peaked χ-profile. Furthermore, it would imply 90 dB damping due to ion-electron energy exchange, corresponding to $\tau_{ie} \approx 5$ ms, which again is unacceptable.

A more credible T-dependence, say $\gamma<1$, would according to (B7) give rise to a relative error in χ^{HP} of <15%, which we do not consider serious in the view of the statistic error of 20%. It would in no way affect the conclusions arrived at in the paper.

Next we examine the term B. For simplicity we assume $\chi \div n^{-1}T^{\gamma}$, so that

$$B = \gamma\chi \frac{1}{T} \frac{\partial^2}{\partial r^2} T + \frac{1}{r} \gamma\chi(\frac{1}{T} \frac{\partial T}{\partial r})$$

Taking $\partial^2 T/\partial r^2$ to be small in the confinement region, a crude estimate of B around $r = \frac{2}{3}a$ is

$$B = \frac{3}{2} \frac{1}{a} \gamma\chi(\frac{1}{T} \frac{\partial T}{\partial r})$$

The resultant contribution to α, $\delta\alpha(B)$, is approximated by (see ref[11]):

$$\delta\alpha(B) = -0.75 \gamma \frac{\chi}{\chi^{HP}} a(\frac{1}{T} \frac{\partial T}{\partial r})$$

Hence apart from not affecting the evaluation of χ^{HP} in the first place, the effect of B an α is 5 times smaller than the effect of A. This again is in agreement with the transport code results, where no significant difference in v_{HP} was observed between the two cases.

REFERENCES

1. Callen J D, Jahns G L, Phys Rev Lett 38 (1977) 971

2. Soler M, Callen J D, Nucl. Fusion 19 (1979) 703

3. Bell J D, Dunlap J L, Pare V K, Callen J D, Howe H C, Lazarus E A, Murakami M, Thomas C E, Nucl Fusion 24 (1984) 997

4. Alladio F, Mazzitelli G, Tuccillo A A, Vlad G, in controlled Fusion and Plasma Physics (Proc. 12th Europ. Conf., Budapest, 1985), 9F-I(1985) 138

5. Tubbing B J D, Barbian E, Campbell D J, Hugenholtz C A J, Niestadt R M, Oyevaar T, Piekaar H W,in controlled Fusion and Plasma Physics (Proc. 12th Europ. Conf., Budapest, 1985) 215

6. Piekaar H W, Goedheer W, Niestadt R M, Stringer T E, Tubbing B J D, 27th meeting of the American Physical Society, Div of Plasma Physics, paper 6P49, in Bull of APS, 30, no 9, San Diego (1985)

7. Sillen R M J, Piekaar H W, Oyevaar Th, Grobunov E P, Bagdasarov A A, Vasin N L, Nucl Fusion 26 (1986) 849.

8. Fredrickson E D, Callen J D, McGuire K, Bell J D, Colchin R J, Efthimion P C, Hill K W, Izzo R, Mikkelsen D R, Motincello D A, Pare V, Taylor G, Zarnstorff M, Nucl Fusion 26 (1986) 849

9. Thomas P R, in Controlled Fusion and Plasma Physics, (Proc 13th Europ. Conf, Schliersee, 1986) 10CI(1986) 37

10. Cordey J G et al., IAEA Conf., Kyoto (1986).

11. Lopes Cardozo N J, Tubbing B J T , Taroni A, Tibone F, to be published

12. Sillen R M J, Piekaar H W, Werner W, Infrared Physics 24, (1984) 511

13. Costley A E et al, Proc 4th Int. Workshop on ECE and ECRH, 1, Rome(1984)

14. Kissel S E et al, Proc. 5th Int Workshop on ECE and ECRH, 65, San Diego(1985).

15. Costley A E et al, in Controlled Fusion and Plasma Physics (Proc. 12th Int Conf., Budapest 1985).

16. Kaye S M, Goldston R J, Nucl Fusion 25 (1985) 65.

17. De Es et al, Equipe TFR, IAEA Conference, Kyoto (1986).

18. Wagner F, Gruber O et al, in Controlled Fusion and Plasma Physics, (Proc. 12th Europ. Conf Budapest, 1985), 9F-I (1985) 335

19. Coppi B, Mazzucato E, Phys Rev Letters 71a (1079) 337

20. Bartlett D et al, in Controlled Fusion and Plasma Physics, (Proc 13th Europ. Conf, Schliersee, 1986)

21. Goedheer W, Nucl Fusion 26 (1986) 1043.

22. Cenacchi G, Taroni A, Proc. 8th Conf on Computational Physics, Eibsee, 1986, 10D (1986) 57

23. Gondhalekar A, et al., IAEA Conf., Kyoto (1986).

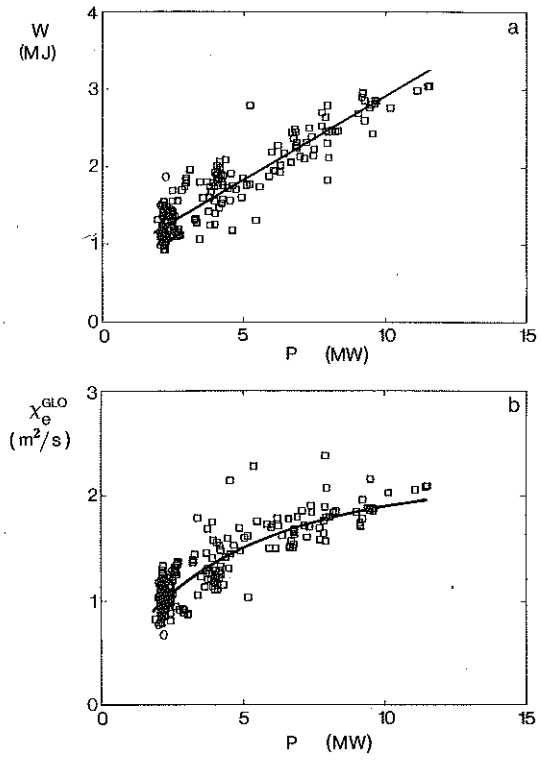

Fig. 1 Global power balance
(a) The total kinetic energy content W as a function of the total input power P, for a selection of JET data: $I_p \approx 3$MA, $B_T \approx 3.4$T, $n_e = (2\text{-}3)10^{19}\text{m}^{-3}$, limiter discharges that are not radiation dominated.
(b) $\chi_e^{GLO} = abP/4W$ as a function of P for the same data set. The full lines in (a) and (b) represent the same off-set linear relation between W and P, corresponding to $\chi_e^{inc} = 2.5\,\text{m}^2/\text{s}$.

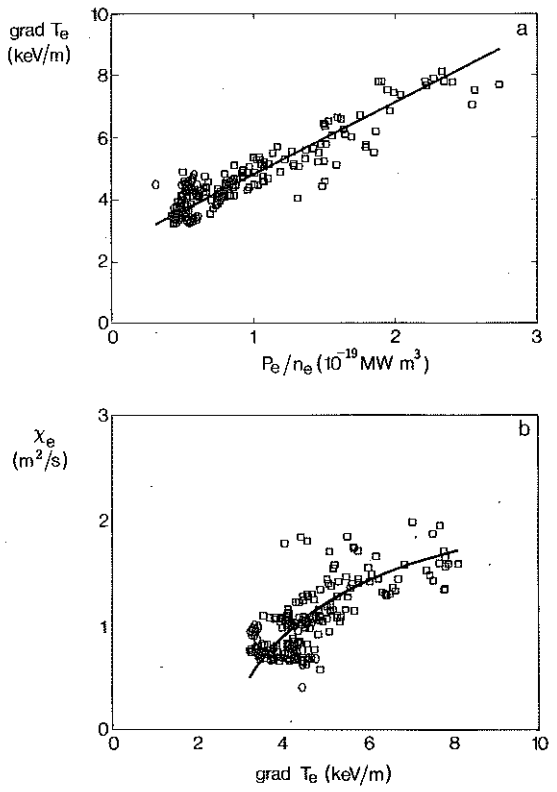

Fig. 2 (a) The T_e-gradient versus the power P_e conducted by the electrons, evaluated at $r = \frac{2}{3}a$
(b) $\chi_e = \text{const.} P_e/(n_e \nabla_r T_e)$ as a function of the T_e-gradient. This figure shows the same selection of data as Fig. 1. The full lines in (a) and (b) represent an off-set linear relation between $\nabla_r T_e$ and P_e/n_e, corresponding to $\chi_e^{inc} = 2.5\,\text{m}^2/\text{s}$.

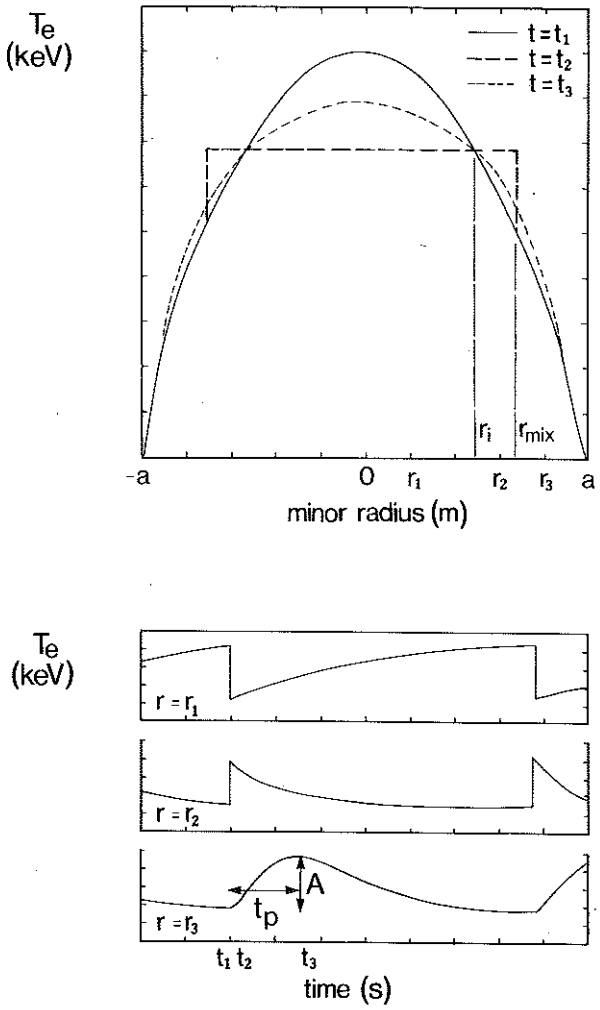

Fig. 3 The evolution of the electron temperature profile during sawtoothing. The upper plot shows profiles just before the collapse of the sawtooth ($t = t_1$), just after ($t = t_2$), and during the rise phase ($t = t_3$). r_{inv} is the inversion radius, r_{mix} the mixing radius. The lower plots show the temperature evolution at radii r_1, r_2, and r_3, as indicated in the upper plot. For $r > r_{mix}$ the heat pulse is observed. The characteristic parameters of the heat pulse are the delay time t_p and the amplitude A.

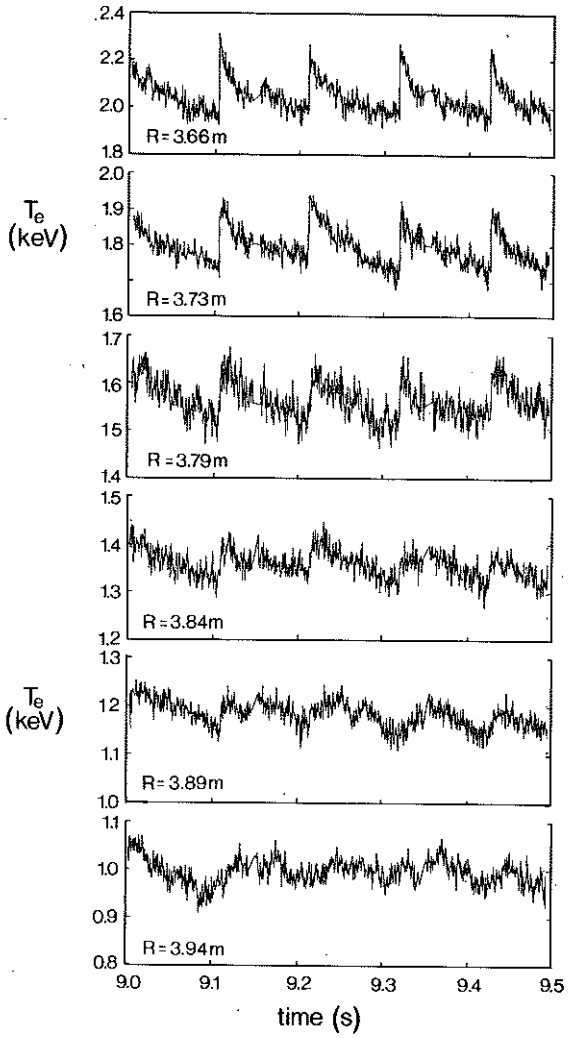

Fig. 4 Measurements of the electron temperature as a function of time, at six radial positions. (JET pulse 7960).

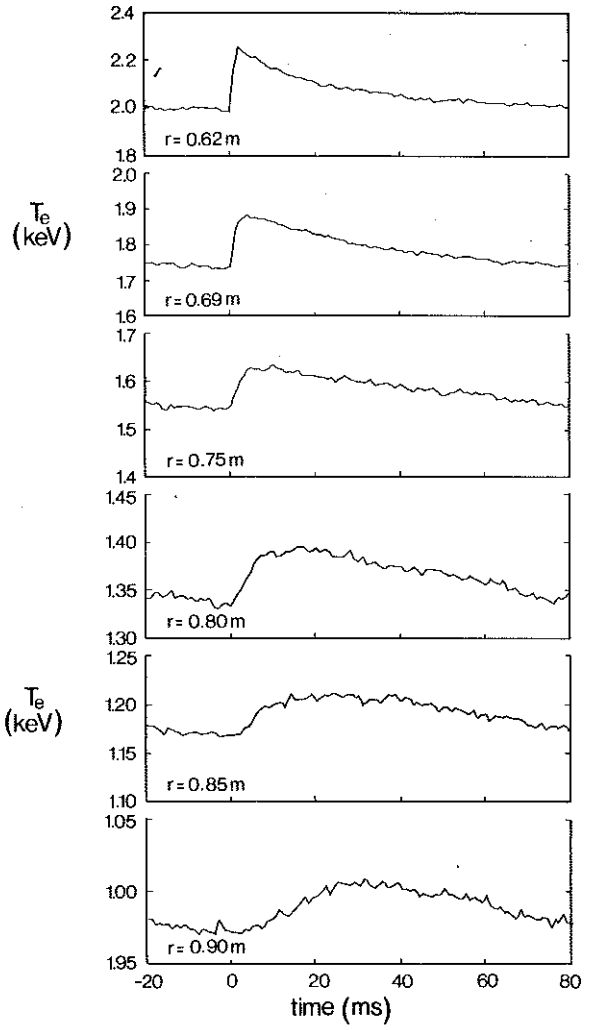

Fig. 5 The averaged heat pulse signals obtained by coherent addition of 22 subsequent sawteeth in the same discharge as Fig. 4: $P = 5\,\mathrm{MW}$.

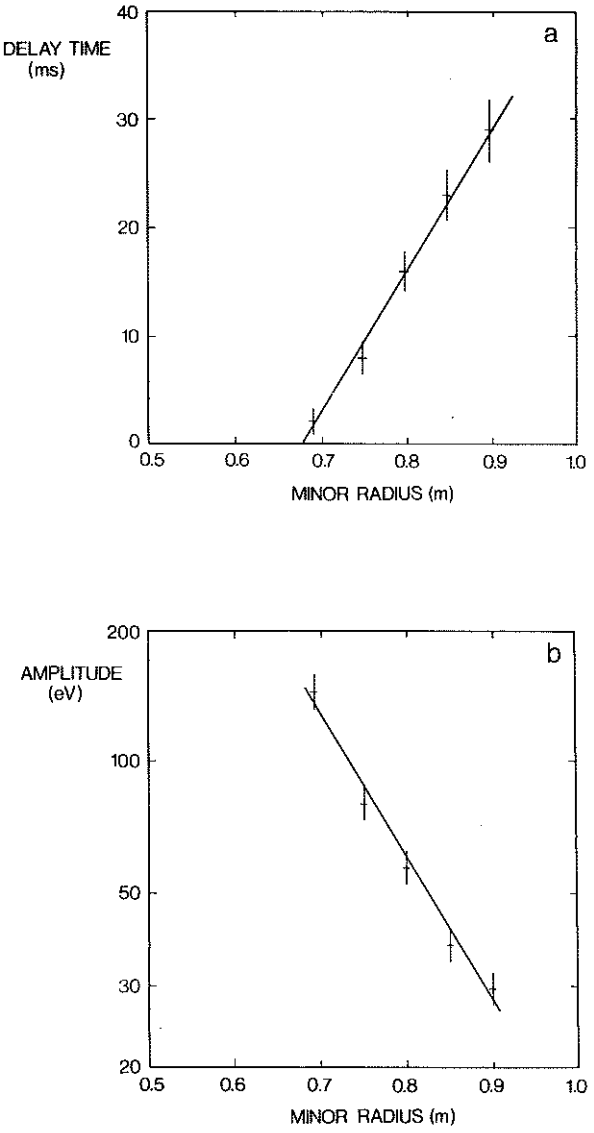

Fig. 6 (a) Pulse delay time t_p as a function of the minor radius. The fitted line yields the heat pulse velocity $v_{HP}^{\dagger} = 7.5\,\mathrm{m/s}$. The limiter is at a minor radius of 1.2 m
(b) Heat pulse amplitude as a function of the minor radius. The fitted line yields the damping rate $\alpha = 43\,\mathrm{dB}$

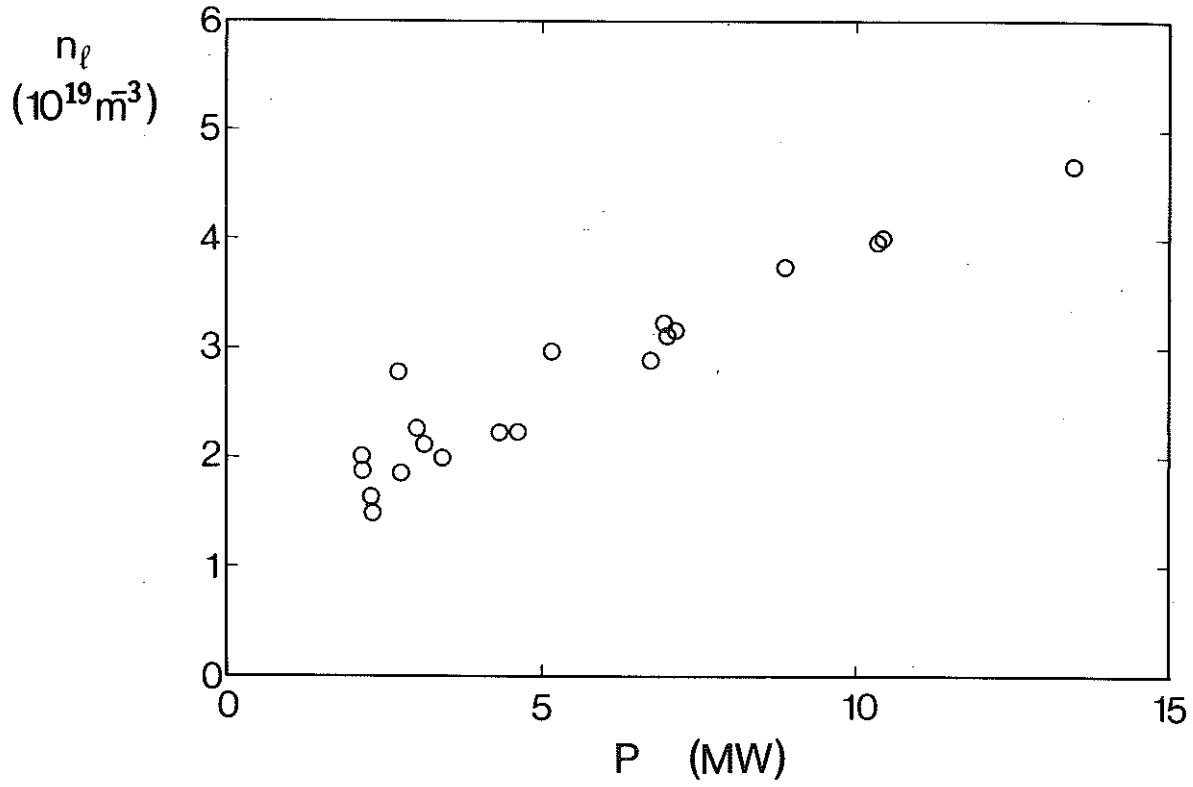

Fig. 7 A constraint on the data set is the correlation between the density and the input power. The plot shows data for all JET pulses of the power scan that are used for the present heat pulse propagation study.

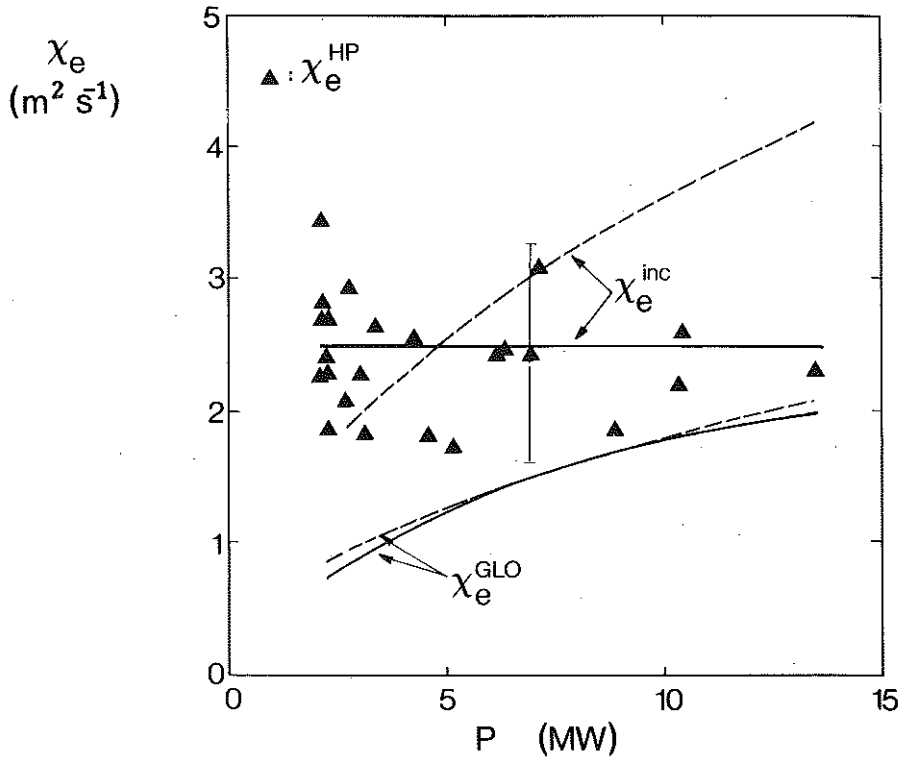

Fig. 8 The measured χ_e^{HP} values as a function of input power P(▲). The full lines depict χ_e^{GLO} and χ_e^{inc} for the off-set linear scaling shown in Figs 1 and 2. The dashed lines represent χ_e^{GLO} and χ_e^{inc} corresponding to the scaling $\tau_E \div P^{-0.5}$ (see Sec. 4). Note that while both scalings yield nearly the same χ_e^{GLO}-values, the off-set linear scaling gives a markedly better fit to the χ_e^{HP} data than the $P^{-0.5}$ scaling.

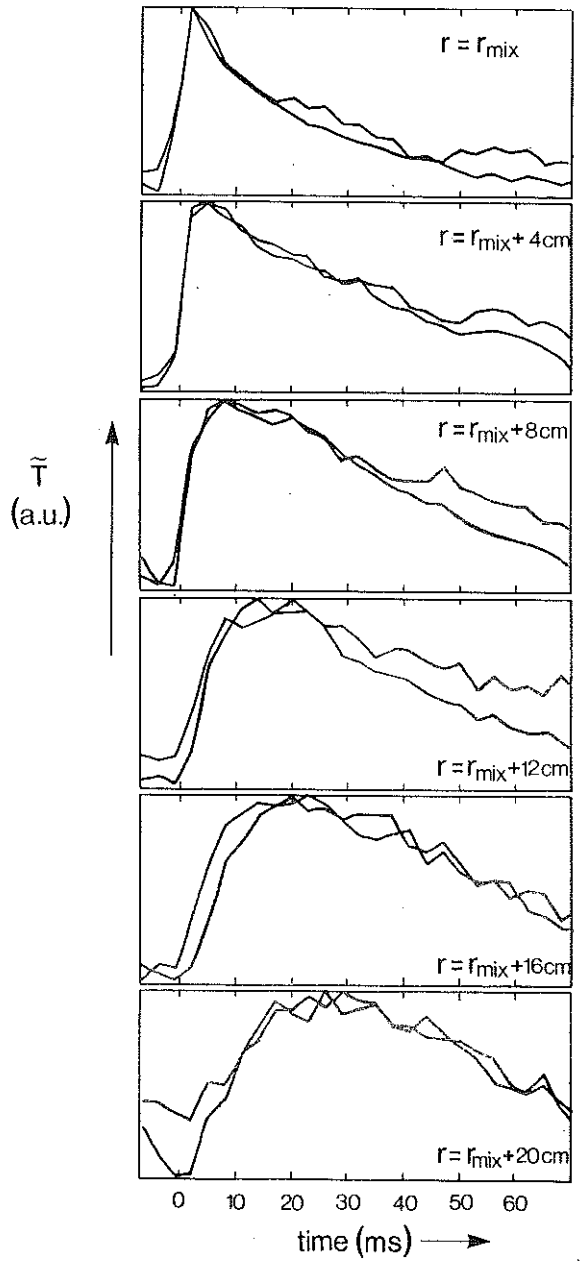

Fig. 9 Averaged heat pulse signals in two discharges, with $P = 2.7\text{MW}$, $n_e = 3.0 \times 10^{19}\text{m}^{-3}$, and $P = 10.4\text{MW}$, $n_e = 4.1 \times 10^{19}\text{m}^{-3}$ respectively. Note that while the input power is quadrupled, the pulse shapes are nearly identical (JET pulses 7959 and 7961).

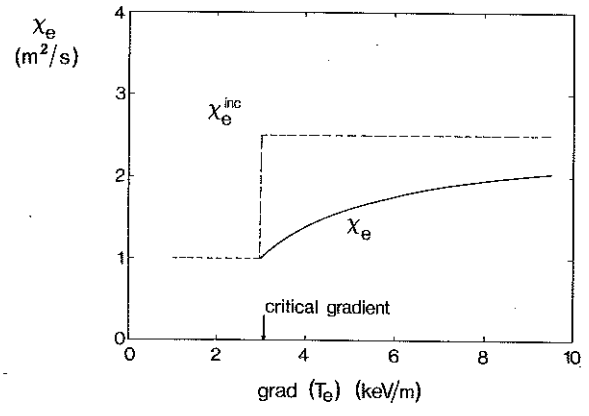

Fig. 10 Sketch of the $\nabla_r T_e$ dependence of χ_e that would model both the heat pulse results and the power balance results. Below the critical gradient and at very high gradients $\chi_e^{HP} \approx \chi_e^{GLO}$, the largest discrepancy is found when $\nabla_r T_e$ is just above critical. Sub-critical gradients may not be obtainable in the normal operating regime of a tokamak, but might be created by means of pellet injection.